February 22, 2022

Chiral superconductivity in cuprates mediated by spin-orbit coupling to spinon superfluidity

Sergei Urazhdin[1]

[1] *Department of Physics, Emory University, Atlanta, USA*

Abstract

We utilize the Hubbard model to demonstrate that doping of the antiferromagnetic parent compounds of cuprate superconductors stabilizes a spin liquid state. Superconductivity in such a state emerges due to the spin-orbit coupling between charge current and superfluidity of spinon condensate, resulting in a chiral relation between the order parameter phase gradient and supercurrent. We propose simple experimental tests for the presented mechanism.

I. INTRODUCTION AND BACKGROUND

Cuprate superconductors such as $Bi_2Sr_2Ca_{n-1}Cu_nO_{2n+4+x}$ (BSCCO) and $YBa_2Cu_3O_{7-x}$ (YBCO) exhibit some of the highest known superconducting transition temperatures T_c [1–3], potentially holding clues to a "holy grail" of condensed matter physics - room-temperature superconductivity (sc) at ambient pressure. sc in these materials cannot be described by the conventional phonon-mediated Bardeen-Cooper-Schrieffer (BCS) mechanism. In classic cuprates such as BiSCO and YBCO, sc is known to be hosted by the CuO planes, which consist of a square lattice of Cu atoms with an oxygen positioned between each pair of the nearest Cu neighbors. In the undoped parent compounds, the $2p$ shell of oxygen is completely filled, while the $4s$ shell of Cu is empty and there is one hole per Cu atom in its $3d$ shell [4]. In the molecular orbital approximation, the tetragonal symmetry of the Cu environment splits its five d-orbitals into a two-fold orbitally degenerate level formed due to the hybridization of the Cu d_{xz}, d_{yz} orbitals with oxygen's p-orbitals, and three orbitally non-degenerate levels derived from the Cu d_{z^2}, d_{xy}, and $d_{x^2-y^2}$ orbitals [5]. Each level is two-fold spin-degenerate. All the orbitals are filled with electrons, except for $d_{x^2-y^2}$, which is half-filled with one hole [5]. Hole representation is utilized throughout this work.

Interactions between holes on the neighboring Cu sites result in the Mott state due to the super-exchange mechanism [6], as outlined below. Hereinafter, the Mott state is defined as an AF-ordered state characterized by a correlation-induced charge excitation gap [7, 8]. The kinetic energy of holes is minimized by hybridization (or hopping in the Hubbard language) between Cu neighbors via oxygen atoms connecting them. If the spins of the holes residing on the neighboring Cu atoms are parallel, their hopping onto the neighbor's site is prohibited by the Pauli principle, raising their kinetic energy. Thus, kinetic energy is minimized in the AF-correlated state between the spins of the holes on the nearest Cu neighbors. In undoped

cuprates with one hole per Cu site, the Coulomb energy increase in the state with two holes on the same site is larger than the kinetic energy reduction due to hopping, which according to the Mott criterion results in the insulating AF state [7]. Electron or hole doping suppresses the insulating Mott state, resulting in the emergence of sc. The normal state above T_c is characterized by anomalous electronic properties such as linear dependence of conductivity on temperature T, which has been attributed to the residual AF correlations [6]. A number of theoretical models exploring the connection between AF correlations and sc, as well as other mechanisms, have been proposed [3, 9–11], but after 35 years of intense research a generally accepted microscopic theory has not yet emerged.

Other prominent unconventional superconductors not described by the BCS theory include strontium titanate (STO) [12], iron-based pnictides [13], and twisted multilayer graphene [14]. The electronic properties and the compositions of these materials are quite diverse. The theories of sc in cuprates tend to focus on the residual AF fluctuations as a possible mechanism of sc [6]. STO is a wide-bandgap semiconductor which exhibits sc at exceptionally low doping level of 10^{17} cm^{-3} [15, 16]. It is a quantum paraelectric [17], so theories of sc in this material tend to focus on electron interactions mediated by the soft ferrodistortive phonon mode [18, 19]. In superconducting pnictides, the Fermi surface is formed by several d-bands [20]. Inter-band electron correlations are believed to play an important role in these and other multi-band superconductors [21, 22]. Some of the proposed mechanisms of sc in twisted multilayer graphene involve inter-valley correlations akin to these multi-band effects [23].

Recent analysis of the electronic properties of STO showed that the bottom of the conduction band in this material is formed by a Kramers doublet of states with unquenched orbital moments and maximal total angular momentum $j = 5/2$ minimizing the spin-orbit coupling (SOC) energy [24]. Coulomb interaction dominant at small carrier density was shown to stabilize a spin-orbit liquid characterized by polaronic-like electron localization. sc in this state can emerge due to the unquenched orbital states stabilized by SOC. Quantum entanglement was then proposed to convert persistent orbital currents into a macroscopic supercurrent. These results established a tentative connection between the mechanisms of sc in STO and multi-band superconductors such as pnictides, where similar unquenched orbital states may be expected due to the SOC-mediated hybridization among the d-bands.

In this work, we demonstrate a similar possibility for cuprates. We revisit the electronic

structure of the CuO plane hosting the valence states, and show that doping stabilizes a spin-orbit liquid state. SOC mediates chiral coupling between superfluidity of chargless excitations of the spin liquid (spinons) and sc. The underlying microscopic mechanism is conversion of persistent orbital currents stabilized by SOC into macroscopic supercurrents, similar to that proposed for STO.

II. MOTT VS SPIN SINGLET STATE IN UNDOPED CUPRATES

In this section, we re-visit the effects of the Mott interaction, which in the Hubbard formalism is described by the Hamiltonian [11]

$$\hat{H} = \hat{H}_{hop} + \hat{H}_{int} = t \sum_{\vec{n},s} \hat{c}^{+}_{\vec{n}+\vec{l},s} \hat{c}_{\vec{n},s} + U \sum_{\vec{n}} \hat{n}_{\vec{n},1/2} \hat{n}_{\vec{n},-1/2}, \tag{1}$$

where the sum is over all the dummy indices. The first term is the kinetic energy described by the hopping parameter t, which is positive for Cu-projected hopping in the CuO_2 plane. The second term describes onsite Coulomb interaction, with $U > 0$. The operator $\hat{c}^{+}_{\vec{n},s}$ creates a hole in the $d_{x^2-y^2}$ molecular orbital (MO) centered on the $\vec{n}^{th}$ Cu site, $\vec{l}$ is a unit vector in the direction of one of the four nearest neighbors along the principal axes, and $\hat{n}_{\vec{n},s} = \hat{c}^{+}_{\vec{n},-s} \hat{c}_{\vec{n},-s}$ is a hole number operator.

Since the interaction energy is dominant in undoped cuprates, the effects of kinetic energy can be analyzed perturbatively [25]. The interaction energy reaches its minimum possible value $E_{int} = 0$ in the states with one hole per site,

$$\psi^{(0)} = \prod_{\vec{n}} \hat{c}^{+}_{\vec{n},s_{\vec{n}}} |0\rangle \tag{2}$$

with spins $s_{\vec{n}}$ uncorrelated among the sites. Any superposition of the states with the form Eq. (2) is a g.s. of $\hat{H}_{int}$, resulting in a massive spin degeneracy partially lifted by hopping. To the second order in $\hat{H}_{hop}$, the energy is

$$E^{(2)} = -\sum_{m} \langle \psi^{(0)} | \hat{H}_{hop} | \psi_m \rangle \langle \psi_m | \hat{H}_{hop} | \psi^{(0)} \rangle / E_m, \tag{3}$$

where ψ_m is an excited many-particle state with interaction energy $E_m > 0$. The term $t\hat{c}^{+}_{\vec{n}+\vec{l},s} \hat{c}_{\vec{n},s}$ in $\hat{H}_{hop}$ annihilates a hole with spin s on site $\vec{n}$ and creates a hole with the same spin on site $\vec{n}+\vec{l}$. Because of the Pauli principle, this is possible only if spins on sites $\vec{n}$ and

$\vec{n}+\vec{l}$ in the state $\psi^{(0)}$ are opposite. Thus, hopping is maximized (hopping energy minimized) in the state with AF-correlated spins on the neighboring sites,

$$\psi^{(1)} = \left[\alpha \prod \hat{c}^{+}_{\vec{n},(-1)^{n_x+n_y}} - \beta \prod \hat{c}^{+}_{\vec{n},(-1)^{n_x+n_y+1}}\right] |0\rangle = \alpha\psi_{AF,+} - \beta\psi_{AF,-} \tag{4}$$

with normalization $|\alpha|^2 + |\beta|^2 = 1$. Here, $\psi_{AF,\pm}$ denote the AF-ordered states with opposite spin polarization.

Higher order hopping contributions lift the $U(2)$ degeneracy of the state Eq. (4) with respect to α, β, resulting in long-range spin entanglement. A system that contains just two sites 1,2 is a special easily tractable case, where such effects appear already in the second order in $\hat{H}_{hop}$. In this case, the second-order energy of the state Eq. (4) is

$$E^{(2)} = -\frac{2t^2}{U}\left[1 + 2Re(\alpha\beta^*)\right], \tag{5}$$

where the dependence on α, β originates from the interference between $\psi_{AF,+}$ and $\psi_{AF,-}$ due to hopping. This energy is minimized in the spin singlet state

$$\psi_{2s} = \frac{1}{\sqrt{2}}\left[\hat{c}^{+}_{1,1/2}\hat{c}^{+}_{2,-1/2} - \hat{c}^{+}_{1,-1/2}\hat{c}^{+}_{2,1/2}\right]|0\rangle, \tag{6}$$

which describes a maximally entangled state of two opposite spins on the neighboring sites.

In systems with N sites, similar interference effects stabilizing long-range entangled spin singlet appear in the N^{th} order of perturbation in $\hat{H}_{hop}$. To facilitate their analysis, we note that each double site occupancy increases the interaction energy by U. Therefore, the dominant intermediate excited states of $\hat{H}_{int}$ in the perturbative expansions with respect to $\hat{H}_{hop}$ contain no more than one doubly-occupied state. Since the unperturbed g.s. Eq. (4) has one hole per site, only even orders of perturbation are finite. Their general form is

$$E^{(2n)} = -\sum_{...,m,m',m'',...} ...\frac{\langle\psi_m|\hat{H}_{hop}|\psi_{m'}\rangle\langle\psi_{m'}|\hat{H}_{hop}|\psi_{m''}\rangle}{U}..., \tag{7}$$

where "..." denote other similar products, ψ_m, $\psi_{m''}$ are states with one hole per site (zero double occupancy), and $\psi_{m'}$ is a state with a single double occupancy and a site with no hole next to it. Since the matrix elements of $\hat{H}_{hop}$ to all the other states besides $\psi_{m'}$ are zero, the sum over m' can be extended to the entire Hilbert state. Eliminating the full projector operator $\sum_{m'}|\psi_{m'}\rangle\langle\psi_{m'}| = \hat{1}$ from Eq. (7), we obtain

$$E^{(2n)} = -\sum_{...,m,m'',...} ...\langle\psi_m|\frac{1}{U}\hat{H}_{hop}\hat{H}_{hop}|\psi_{m''}\rangle.... \tag{8}$$

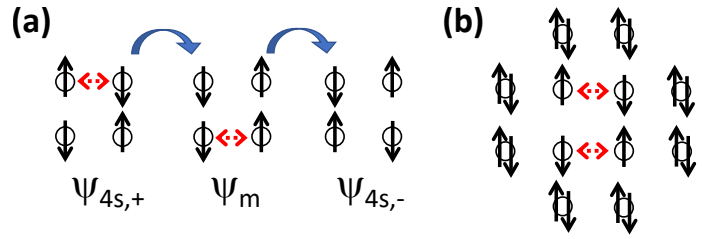

Figure 1. Hopping-induced mixing between AF states. (a) For a 2×2 system with 1 hole per site, the AF states $\psi_{4s,+}$ and $\psi_{4s,-}$ are mixed via two neighboring spin exchanges, i.e. in the 4th order in $\hat{H}_{hop}$. (b) For a 2×2 plaquette with one hole site surrounded by sites with 2 holes in an extended system, only 4 sites are AF-correlated. AF states become mixed to the same order in hopping as in (a).

Thus, analysis of the effects of H_{hop} is simplified by considering the effective second-order hopping operator $\hat{H}^{(2)}_{hop} = -\frac{1}{U}\hat{H}_{hop}\hat{H}_{hop}$ on the subspace of states with a single hole per site.

The only non-vanishing matrix elements on this subspace describe hopping of a hole with spin s from site $\vec{n}$ onto the neighboring site $\vec{n}+\vec{l}$, and hopping back of the hole either with the same or opposite spin,

$$\hat{H}^{(2)}_{hop} = -\frac{t^2}{U}\sum \hat{c}^{+}_{\vec{n},s'}\hat{c}_{\vec{n}+\vec{l},s'}\hat{c}^{+}_{\vec{n}+\vec{l},s}\hat{c}_{\vec{n},s}. \tag{9}$$

Using the relation $\hat{n}_{\vec{n},s}+\hat{n}_{\vec{n},-s}=1$ valid on the subspace with one hole per site, this equation is transformed into

$$\hat{H}^{(2)}_{hop} = \hat{H}_{AF} + \hat{H}_{ex} = -V\sum \hat{n}_{\vec{n},s}\hat{n}_{\vec{n}+\vec{l},-s} - V\sum \hat{c}^{+}_{\vec{n},s}\hat{c}^{+}_{\vec{n}+\vec{l},-s}\hat{c}_{\vec{n},-s}\hat{c}_{\vec{n}+\vec{l},s}, \tag{10}$$

where we define $V = \frac{t^2}{U} > 0$.The first term on the right describes AF coupling of the neighboring spins, while the second term exchanges them.

The usefulness of the second-order Hamiltonian Eq. (10) is illustrated in Fig. 1(a) for a 2×2 site system. In this case, interference between $\psi_{AF,+}$ and $\psi_{AF,-}$ stabilizing the spin singlet g.s. arises in the 2^{nd} order in $\hat{H}_{ex}$ (4^{th} order in $\hat{H}_{hop}$). In the example in Fig. 1(a), the two top spins are exchanged first. Exchange between the two bottom spins then converts $\psi_{AF,+}$ into $\psi_{AF,-}$. The resulting second-order in $\hat{H}_{ex}$ correction to the energy of the state Eq. (4) is $-2t^4 Re(\alpha\beta^*)/U^3$. Each of the three other intermediate states provides the same energy correction, stabilizing a spin-singlet state characterized by $\alpha = \beta$ with energy $E_{4s} = -8t^4 Re(\alpha\beta^*)/U^3$ below $E_{AF} = 0$ of the AF state.

By extension, the g.s. a system containing N sites is a long-range entangled singlet

$$\psi_{Ns} = \frac{1}{\sqrt{2}}\left[\prod \hat{c}^{+}_{\vec{n},(-1)^{nx+ny}} - \prod \hat{c}^{+}_{\vec{n},(-1)^{nx+ny+1}}\right]|0\rangle = \frac{1}{\sqrt{2}}[\psi_{AF,+} - \psi_{AF,-}] \tag{11}$$

with energy $E_{Ns} \approx -2^{N/2+1}(N/2)!t^N Re(\alpha\beta^*)/U^{N-1}$, where N is assumed to be even, and the numeric factor is calculated by neglecting the boundary effects in the limit of large N.

The relation between the phases and amplitudes of the two AF components of the singlet g.s. Eq. (11) is stabilized by the weak N^{th} order interference effects, which can be suppressed by thermal fluctuations and other perturbations resulting in dephasing of the many-particle wavefunction. In particular, quenched or fluctuating local magnetic fields favor one AF component over the other, which may be expected to result in the spontaneous transition to AF-ordered state characterized by $\alpha = 0$, $|\beta| = 1$ or $\beta = 0$, $|\alpha| = 1$ in Eq. (4).

The same perturbations also suppress long-range AF correlations, effectively reducing N, and thus enhancing the interference effects stabilizing the spin singlet. This is illustrated for a hole-doped system in Fig. (1)(b), where a 2×2 plaquette with 1 hole per site is surrounded by sites with two holes each. In this configuration, the singlet state of the plaquette is stabilized in the 2^{nd} order in $\hat{H}_{ex}$. Configurations evolve as the itinerant holes hop, but the overall effect of singlet enhancement remains. In the next section we analyze the effects of short-range entanglement expected to be dominant in this limit.

III. MEAN-FIELD APPROXIMATION FOR THE SPIN LIQUID

The mean-field approximation of the BCS theory describes an entangled spin singlet state of two electrons with opposite wavevectors [26]. For the spin singlet state discussed above, the mean-field approximation similarly captures the effects of two-particle singlet entanglement, as shown next. Singlet correlations are described by the order parameter

$$\Delta_{\vec{l}}(\vec{n}) = V\langle \hat{c}_{\vec{n},1/2}\hat{c}_{\vec{n}+\vec{l},-1/2} - \hat{c}_{\vec{n},-1/2}\hat{c}_{\vec{n}+\vec{l},1/2}\rangle, \tag{12}$$

The interaction results in the dominance of states with a single hole per site. We now consider the projection of the Hamiltonian on he subspace formed by such states. The interaction energy vanishes, leaving only $H^{(2)}_{hop}$, which can be written as

$$\hat{H}^{(2)}_{hop} = V\sum(\hat{c}^{+}_{\vec{n},1/2}\hat{c}^{+}_{\vec{n}+\vec{l},-1/2} - \hat{c}^{+}_{\vec{n},-1/2}\hat{c}^{+}_{\vec{n}+\vec{l},1/2})(\hat{c}_{\vec{n},1/2}\hat{c}_{\vec{n}+\vec{l},-1/2} - \hat{c}_{\vec{n},-1/2}\hat{c}_{\vec{n}+\vec{l},1/2}) \tag{13}$$

Inserting the identity

$$\hat{c}_{\vec{n},+}\hat{c}_{\vec{n}+\vec{l},-1/2} - \hat{c}_{\vec{n},-}\hat{c}_{\vec{n}+\vec{l},1/2} = \Delta_{\vec{l}}(\vec{n}) + [\hat{c}_{\vec{n},+}\hat{c}_{\vec{n}+\vec{l},-1/2} - \hat{c}_{\vec{n},-}\hat{c}_{\vec{n}+\vec{l},1/2} - \Delta_{\vec{l}}(\vec{n})] \tag{14}$$

and a similar identity for creation operators into the Hamiltonian, and keeping only linear terms in fluctuations [terms in parentheses in Eq. (14)], we obtain mean-field Hamiltonian

$$\begin{aligned}\hat{H}_{mf} = &\sum \frac{|\Delta_{\vec{l}}|^2}{V} - \Delta^*_{\vec{l}}(\hat{c}_{\vec{n},1/2}\hat{c}_{\vec{n}+\vec{l},-1/2} - \hat{c}_{\vec{n},-1/2}\hat{c}_{\vec{n}+\vec{l},1/2}) \\ &+\Delta_{\vec{l}}(\hat{c}^+_{\vec{n},1/2}\hat{c}^+_{\vec{n}+\vec{l},-1/2} - \hat{c}^+_{\vec{n},-1/2}\hat{c}^+_{\vec{n}+\vec{l},1/2}),\end{aligned} \tag{15}$$

where the site dependence is dropped assuming that $\Delta_{\vec{l}}$ are weakly position-dependent. In the momentum representation, Eq. (15) becomes

$$\hat{H}_{mf} = \frac{2N(|\Delta_x|^2 + |\Delta_y|^2}{V} - 2\sum_{\vec{k},\vec{l}}[\Delta^*_{\vec{l}}\hat{c}_{\vec{k},1/2}\hat{c}_{-\vec{k},-1/2} - \Delta_{\vec{l}}\hat{c}^+_{\vec{k},1/2}\hat{c}^+_{-\vec{k},-1/2}]\cos(\vec{k}\vec{l}a), \tag{16}$$

where the first term is simplified using $\Delta_{-\vec{l}} = \Delta_{\vec{l}}$. To diagonalize this Hamiltonian, we perform the canonical transformation [26]

$$\hat{c}_{\vec{k},s} = u_{\vec{k},s}\gamma_{\vec{k},\sigma} + v^*_{\vec{k},s}\gamma^+_{-\vec{k},-\sigma}, \tag{17}$$

where $\gamma^+_{\vec{k},\sigma}$ is the Bogolyubovon creation operator indexed with pseudo-spin $\sigma = \pm$, and $u_{\vec{k},s}$, $v_{\vec{k},s}$ are the transformation coefficients. The commutation relations among γ, γ^+ impose the conditions

$$|u_{\vec{k},\sigma}|^2 + |v_{\vec{k},\sigma}|^2 = 1,\ u_{\vec{k},\sigma}v^*_{-\vec{k},-\sigma} = -u_{-\vec{k},-\sigma}v^*_{\vec{k},\sigma}. \tag{18}$$

The Hamiltonian can be diagonalized if Δ_x and Δ_y have the same complex phase. They can then be set real and positive by an appropriate gauge. In this case, the Hamiltonian is diagonalized by $u_{\vec{k},s} = -v_{\vec{k},1/2} = v_{\vec{k},-1/2} = 1/\sqrt{2}$,

$$\hat{H}_{mf} = \frac{2N(|\Delta_x|^2 + |\Delta_y|^2)}{V} - 8\sum_{\vec{k}}(\Delta_x\cos k_x a + \Delta_y \cos k_y a)(1 - \gamma^+_{\vec{k},+}\gamma_{\vec{k},+} - \gamma^+_{\vec{k},-}\gamma_{\vec{k},-}). \tag{19}$$

Its excitation spectrum is independent of the pseudo-spin,

$$\epsilon(\vec{k}) = 8(\Delta_x\cos k_x a + \Delta_y \cos k_y a). \tag{20}$$

The excitation with pseudo-spin σ is an equal-amplitude superposition of a hole with spin $\sigma/2$ and an electron in the state with spin $-\sigma/2$. Thus, Bogolyubovons are chargeless

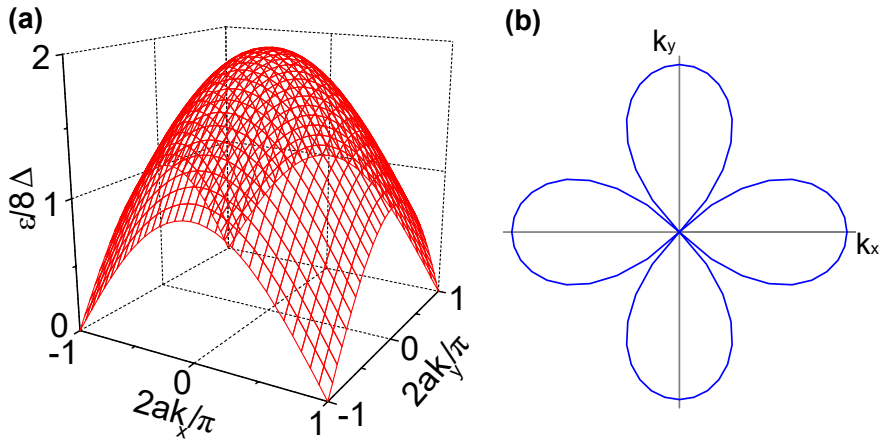

Figure 2. (a) Spinon spectrum in the spin liquid state. (b) Directional dependence of excitation gap.

spin-1/2 fermions, the spinons [27]. In the chosen gauge (real positive Δ), the pseudo-spin σ is the projection of spinon spin on the x-axis. For the gauge $\Delta = e^{i\varphi}|\Delta|$, σ describes spin projection on the in-plane direction rotated by angle φ relative to the x-axis.

Finite Δ_x, Δ_y break the equivalence between neighboring sites in x and y directions, respectively, doubling the lattice constant. Thus, the folded Brillouin Zone (BZ) is a square extending from $-\pi/2a$ to $\pi/2a$ in k_x and k_y directions. As shown in Fig. 2, the spectrum is gapless, i.e. the condensed state is a spin liquid [28]. The directional dependence of the gap, Fig. 2(a) is consistent with the measured anisotropy of the excitation gap in cuprates [29]. In the presented analysis, this dependence is not directly related to the directional dependence of the orbital $d_{x^2-y^2}$ that dominates the valence states. The spectrum is linear at small energies near the four equivalent corners of BZ at $\vec{k} = (\pm\pi/2a, \pm\pi/2a)$, i.e. it contains four quadrants of a Dirac point at the corners of BZ. We show below that the properties of excitations are singular at the Dirac point.

Using the definition Eq. (12) we obtain the self-consistency conditions for Δ_x, Δ_y,

$$\begin{aligned} N\Delta_x &= V\langle \sum_{\vec{k}} \cos k_x a (2 - \gamma^+_{\vec{k},+}\gamma_{\vec{k},+} - \gamma^+_{\vec{k},-}\gamma_{\vec{k},-})\rangle \\ N\Delta_y &= V\langle \sum_{\vec{k}} \cos k_y a (2 - \gamma^+_{\vec{k},+}\gamma_{\vec{k},+} - \gamma^+_{\vec{k},-}\gamma_{\vec{k},-})\rangle \end{aligned} \tag{21}$$

which at $T = 0$ are satisfied by $\Delta_x = \Delta_y \equiv \Delta = V/\pi$. Thus, in contrast to the resonating valence bond model [6, 9], pairwise singlet entanglement described by the order parameter Δ is isotropic. The total energy of the g.s. described by Eq. (19) is $E_{g.s.} = -6NV/\pi^2$, which in

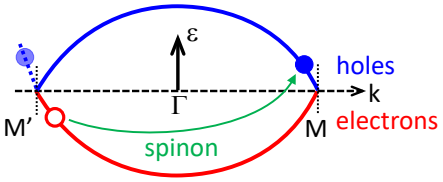

Figure 3. Excitation spectrum along the Γ-M direction of BZ. Spinon is a superposition of a hole (filled symbols) with electron (open symbol). The spectral branch required to describe holes (dashed) disappears in the folded BZ.

contrast to the spin-singlet correlations in BCS is satisfied at any V. This result reflects the single hole per site approximation underlying the model, which neglects the kinetic energy gain due to the hole delocalization at $\Delta = 0$.

At finite T, the mode populations $n_{\vec{k},\sigma} = \langle \gamma^+_{\vec{k},\sigma} \gamma_{\vec{k},\sigma} \rangle$ become finite, approaching 1/2 at $T \gg V/k_B$, where k_B is the Boltzmann constant. According to Eq. (21), finite values of Δ remain possible even at such high temperatures, demonstrating that local singlet correlations are robust with respect to thermal fluctuations. However, at such high temperatures the single hole per site approximation underlying these results becomes invalid.

IV. ELECTRONIC PROPERTIES OF THE DOPED SPIN-LIQUID STATE

An argument illustrated by Fig. 1(b) suggests that doping reduces the effective size of entangled regions, lowering the singlet energy relative to the AF-ordered states. In the preceding section, we supported this argument with mean-field analysis valid in the limit of short-range entanglement at sufficiently large doping. Here, we analyze the electronic properties of the dopant holes in the spin singlet state stabilized by doping.

A spinon is a superposition of a hole and an electron with opposite wavevectors and spins [Fig. 3], as follows from

$$\hat{\gamma}^+_{\vec{k},\sigma} = \frac{1}{\sqrt{2}} (\hat{c}^+_{\vec{k},\sigma/2} + \sigma \hat{c}_{-\vec{k},-\sigma/2}). \tag{22}$$

In contrast, a charge excitation would be produced by a superposition of a hole with a hole that resides on the branch of the spectrum that disappears in the condensed state due to the BZ folding [Fig. 3], making it difficult to describe charges within the mean-field model.

To resolve this difficulty, consider a singlet of two zero-energy holes with wavevectors $\vec{k}_M = (\pi/2a, \pi/2a)$, $\vec{k}_{M'} = -\vec{k}_M$ at the two equivalent opposite corners of folded BZ added

to the spinon vacuum $|0_\gamma\rangle$,

$$\psi_{2hs} = \frac{1}{\sqrt{2}}(\hat{c}^+_{\vec{k}_M,1/2}\hat{c}^+_{\vec{k}_{M'},-1/2} - \hat{c}^+_{\vec{k}_M,-1/2}\hat{c}^+_{\vec{k}_{M'},1/2})|0_\gamma\rangle, \tag{23}$$

Using the equivalence of $\vec{k}_M$ and $\vec{k}_{M'}$, this expression is transformed into

$$\psi_{2hs} = \frac{1}{\sqrt{2}}(\hat{\gamma}^+_{\vec{k}_M,+}\hat{\gamma}^+_{\vec{k}_M,-} - \hat{\gamma}^+_{\vec{k}_M,-}\hat{\gamma}^+_{\vec{k}_M,+})||0_\gamma\rangle. \tag{24}$$

We determine the order parameter in this state using Eq. (21),

$$\Delta = V(\frac{1}{\pi} - \frac{2}{N}). \tag{25}$$

This result shows that the state with a singlet of two spinons at the corners of folded BZ can be equivalently described as a spin singlet of two holes akin to the Rice-Zhang singlet [5], with the order parameter slightly reduced by doping. While the presented model cannot naturally incorporate more than two holes, additional charges can be approximately accounted for by using the following argument. Two holes are allowed by our model for a system with size N. Thus, four holes can be accommodated by dividing this system in two parts, etc. In this approach, the doping level is $2/N$. All of these holes form singlet pairs, and according to Eq. (25) reduce the condensate amplitude in proportion to doping. The collapse of singlet correlations at large doping is qualitatively captured by Eq. (25) but not correctly described by this equation, because the above analysis does not incorporate quantum charge fluctuations. This collapse signifies the transition from a "strange" metal where charge is carried by singlet hole pairs to the uncorrelated metal state, consistent with the experimental observations [3].

V. EFFECTS OF SOC

In this section, we show that SOC produces an anomalous velocity of band states that translates into chiral currents carried by SOC spinons despite their vanishing charge. Chiral SOC-induced transport has been extensively analyzed in the context of anomalous and spin Hall effects [30, 31]. Microscopically, such effects in cuprates likely arise due to the d-band hybridization mediated by the CuO plane distortions and/or coupling to the environment of these planes [32, 33]. This band mixing allows for finite matrix elements of SOC coupling between $d_{x^2-y^2}$ and d_{xy}, stabilizing the states $d_{pm2} = (d_{x^2-y^2} \mp id_{xy})/\sqrt{2}$ with finite orbital

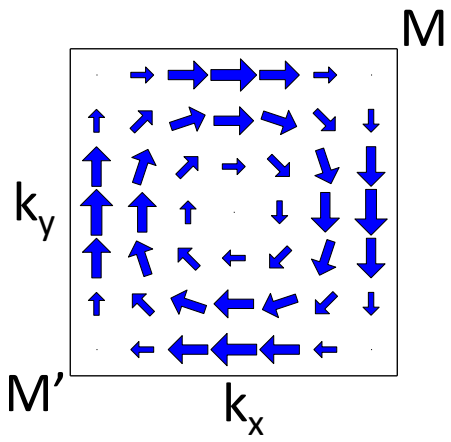

Figure 4. Distribution of SOC-induced anomalous velocities of single-hole states with $s = 1/2$. The directions for $s = -1/2$ are opposite.

moment projections $m = \pm$ coupled to spin. Their detailed analysis is beyond the scope of this work.

In the Hubbard formalism, these SOC effects projected on the $d_{x^2-y^2}$ orbitals can be described by chiral spin-dependent next-neighbor hopping Hamiltonian [34, 35]

$$H'_{hop} = it' \sum_{\vec{n},\vec{l},\vec{l}',s} s(l_x l'_y - l_y l'_x) \hat{c}^+_{\vec{n}+\vec{l},s} \hat{c}_{\vec{n}+\vec{l}',s}, \tag{26}$$

where t' is proportional to the SOC parameter of Cu, and $\vec{l}$, $\vec{l}'$ are unit vectors along one of the four principal directions. The single-particle dispersion is not affected by this chiral contribution. In contrast, the particle velocity acquires a circulating anomalous component [31, 36]

$$\vec{v}_{an}(\vec{k}, s) = \langle \psi_{\vec{k},s} | \frac{[\hat{H}'_{hop}, \vec{\hat{r}}]}{i\hbar} | \psi_{\vec{k},s} \rangle = \frac{8at's}{\hbar} (\sin ak_y \cos ak_x, -\sin ak_x \cos ak_y), \tag{27}$$

where $\vec{\hat{r}} = a \sum \vec{n} \hat{c}^+_{\vec{n},s} \hat{c}_{\vec{n},s}$ is the coordinate operator. This equation describes current that circulates around the BZ [Fig. 4], and reverses upon reversal of either $\vec{k}$ or s.

VI. CHIRAL SC COUPLED TO SPINON SUPERFLUIDITY

In the BCS theory, a gauge-symmetric complex order parameter $\Delta = |\Delta| e^{2i\varphi}$ describes Cooper pairs formed by spin singlets of electrons with opposite wavevectors. A gradient $\nabla\varphi = \vec{q}$ is associated with a shift of the momentum of each electron in a Cooper pair by

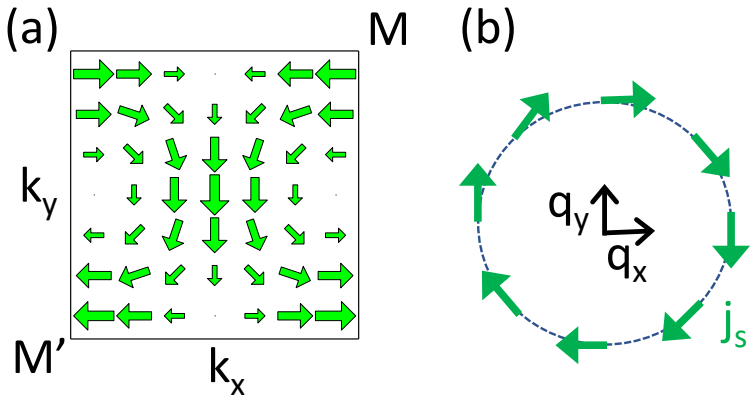

Figure 5. (a) Current density carried by spinons in the presence of a condensate phase gradient $\vec{q} \parallel \vec{e}_x$. (c) Chiral relationship between the direction of $\vec{q}$ and $\vec{j}_s$.

$\vec{q}$, which carry a charge supercurrent [26]. For the spinon condensate, phase gradient of Δ describes superflow of chargeless spinons, which is not necessarily associated with a charge current.

To analyze the effects of phase gradient of spinon condensate, we return to the canonical transformation that defines the relationship between charged particles and spinons. In Section IV, this transformation was performed under the assumption that Δ is positive and real. For $\Delta = e^{2i\varphi}|\Delta|$, the canonical transformation in the coordinate representation becomes

$$u_{\vec{n},s} = e^{i\varphi}/\sqrt{2},\ v_{\vec{n},-1/2} = -v_{\vec{n},1/2} = e^{-i\varphi}/\sqrt{2}, \tag{28}$$

which entails the relation

$$\hat{c}_{\vec{k},1/2} = \frac{e^{i\varphi}}{\sqrt{2}}(\gamma_{\vec{n},+} - \gamma^{+}_{\vec{n},-}),\ \hat{c}_{\vec{k},-1/2} = \frac{e^{i\varphi}}{\sqrt{2}}(\gamma_{\vec{n},-} + \gamma^{+}_{\vec{n},+}) \tag{29}$$

between the spinon and the particle operators. The phase can be absorbed in the definition $\hat{c}'_{\vec{k},s} = e^{-i\varphi}\hat{c}_{\vec{k},s}$, so that all the relationships of the previous sections remain the same by replacing $\hat{c}$ with $\hat{c}'$.

We now consider anomalous velocity associated with chiral hopping Eq. (26) in the state characterized by finite a phase gradient $\nabla\varphi = \vec{q}$. Following the same approach as in the previous section, we obtain

$$\vec{v}_{an}(\vec{k}, s) = \frac{8at's}{\hbar}[\sin a(k_y + q_y)\cos a(k_x + q_x), -\sin a(k_x + q_x)\cos a(k_y + q_y)]. \tag{30}$$

In the semiclassical limit at small $\vec{q}$, spinons are still described by the equal-weight superpositions of electrons with spins s and wavevectors $\vec{k}$ and electrons with spins $-s$ and

wavevectors $-\vec{k}$. However, a finite $\vec{q}$ breaks the symmetry between these states, so that their contributions to charge current density carried by a spinon

$$\vec{j}(\vec{k},\sigma) = \frac{e}{2Na^2}(\vec{v}_{an}(\vec{k},s) - \vec{v}_{an}(-\vec{k},-s)) \tag{31}$$

no longer cancel,

$$\begin{aligned} j_x(\vec{k},\sigma) &\approx \frac{4t'e\sigma}{\hbar aN}[-\sin(ak_y)\sin(ak_x)q_x + \cos(ak_y)\cos(ak_x)q_y] \\ j_y(\vec{k},\sigma) &\approx \frac{4t'e\sigma}{\hbar aN}[-\cos(ak_x)\cos(ak_y)q_x - \sin(ak_x)\sin(ak_y)q_y] \end{aligned} \tag{32}$$

The resulting distribution of current carried by "phase-twisted" spinons is shown in Fig. 5(a) for $\sigma = +$ and $\vec{q}$ along the x-axis.

As is well-known for gauge-symmetric order parameters [26, 37], superflow associated with the gradient of condensate phase is carried by pairs of spinons characterized by pseudo-spin $\sigma = +$ and wavevector $\vec{k}+\vec{q}$, and pseudo-spin $\sigma = -$ and wavevector $-\vec{k}+\vec{q}$. Since Eq. (34) is antisymmetric with respect to both spin and $\vec{q}$, the current densities carried by each spinon in a pair add. The total current density carried by such a spinon pair is

$$\vec{j}_c(\vec{k}) = \vec{j}(\vec{k},+) + \vec{j}(-\vec{k},-) = 2\vec{j}(\vec{k},+). \tag{33}$$

The total current density carried by the condensate is the sum over all such pairs,

$$j_c = \frac{|\Delta|}{V}\sum_{\vec{k}} \vec{j}_c(\vec{k}) = \frac{8t'e|\Delta|}{\hbar\pi^2 aV}(q_y, -q_x), \tag{34}$$

which describes a chiral relationship between the gradient of the order parameter phase and the supercurrent direction, Fig. 5(b).

VII. CONCLUSIONS

In this work, we developed a model of sc in cuprates mediated by a combination of spin-orbit interaction and correlation effects. We utilized two-particle mean-field analysis to show that in the presence of dopant holes, Mott interaction stabilizes a spin liquid state characterized by a gapless spectrum of chargeless excitations, the spinons. Spin-orbit interaction results in chiral currents that mediate coupling between spin superfluidity of spinon condensate and sc. Since spin-orbit coupling is central to the proposed mechanism, we predict that

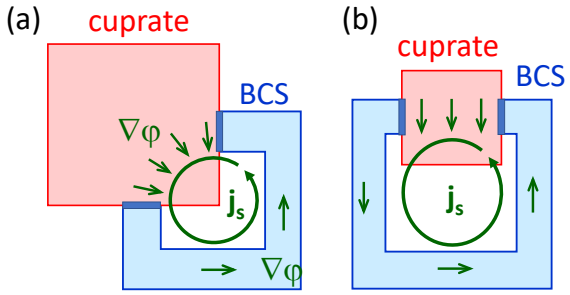

Figure 6. (a) Schematic of the corner Josephson junction experiment, with arrows showing the gradient of sc phase associated with supercurrent j_s. (b) Proposed opposite-junction experiment, which is expected to exhibit an interference pattern similar to that of the corner junction.

isoelectronic substitution of Cu with Ag should enhance critical current due to the increase of the chiral current around the M-point. Meanwhile, critical magnetic field should decrease due to the more efficient suppression of pseudo-spin singlet state characterized by larger magnetic moments involved in the spin-orbit singlet state.

Our analysis is consistent with the unusual symmetries and excitation properties of cuprate superconductors. At light doping, the spin-orbit liquid state is a correlated metal where charge is carried by spin singlet hole pairs akin to Rice-Zhang singlets [5], with wavevectors at the corners of the folded Brillouin zone. The singlet condensate is expected to collapse at large doping, resulting in the transition to the uncorrelated metal state. The condensate amplitude is maximized along the x and y axes, with nodes along the diagonals [Fig. 2(b)]. This dependence resembles the $d_{x^2-y^2}$ wavefunction, but in our model results from the gap anisotropy of spinon spectrum. Based on our model, we suggest that the pseudo-gap observed above T_c is associated with the local Mott correlations that open a spectral gap without the long-range coherence of spinon condensate necessary for sc.

One of the hallmarks of sc in cuprates is the apparent reversal of the condensate phase upon rotation between x and y axes interpreted as the $d_{x^2-y^2}$ symmetry of the order parameter [29]. For instance, in the famous corner junction experiment [38], a square cuprate sample is contacted via Josephson junctions on two neighboring sides by a BCS superconductor, forming a loop [Fig. 6(a)]. The phase gradients of the order parameter associated with a supercurrent flowing around the loop are shown in Fig. 6 by green arrows. Because of the chiral relationship between the phase gradient and the supercurrent direction, in the absence of magnetic flux the supercurrent in the cuprate is maximized in this geometry by zero

phase difference between the two neighboring sides. Meanwhile, in the BCS superconductor it is maximized by the maximum phase difference, resulting in a minimum of critical current at zero magnetic flux. The phase relationships between the two junctions are periodically modulated by the magnetic flux through the loop, resulting in the interference pattern characterized by a minimum of the critical current at zero magnetic flux. A simple test for the presented alternative interpretation is the opposite-side double-junction [Fig. 6(b)], which should exhibit an interference pattern similar to that of the corner junction.

Microscopically, the presented mechanism can be interpreted as a consequence of persistent orbital currents enabled by admixture of other d-bands to the $d_{x^2-y^2}$ band and coupled to spin by spin-orbit interaction. Spinon entanglement then effectively "rectifies" the circulating orbital currents, resulting in a macroscopic supercurrent. This mechanism is similar to the one recently proposed for STO, and is likely relevant to other unconventional superconductors [24].

This work was supported by the NSF Awards ECCS-1804198 and ECCS-2005786. The idea of superconductivity mediated by unquenched orbitals was conceived with support from the DOE BES Award # DE-SC0018976.

---

[1] J. G. Bednorz and K. A. Muller, Possible High Tc superconductivity in the BaLaCuO system, Zeitschrift fur Physik B Condensed Matter **64**, 189 (1986).

[2] J. G. Bednorz and K. A. Müller, Perovskite-type oxides—the new approach to high-T_c superconductivity, Rev. Mod. Phys. **60**, 585 (1988).

[3] N. M. Plakida, *High-temperature cuprate superconductors : experiment, theory, and applications* (Springer-Verlag, Berlin Heidelberg, 2010).

[4] Y. Guo, J.-M. Langlois, and W. A. Goddard, Electronic structure and valence-bond band structure of cuprate superconducting materials, Science **239**, 896 (1988).

[5] F. C. Zhang and T. M. Rice, Effective hamiltonian for the superconducting cu oxides, Phys. Rev. B **37**, 3759 (1988).

[6] P. W. Anderson, The resonating valence bond state in la¡sub¿2¡/sub¿cuo¡sub¿4¡/sub¿ and superconductivity, Science **235**, 1196 (1987).

[7] N. F. MOTT, Metal-insulator transition, Rev. Mod. Phys. **40**, 677 (1968).

[8] D. Belitz and T. R. Kirkpatrick, The anderson-mott transition, Rev. Mod. Phys. **66**, 261 (1994).

[9] S. A. Kivelson, D. S. Rokhsar, and J. P. Sethna, Topology of the resonating valence-bond state: Solitons and high-T_c superconductivity, Phys. Rev. B **35**, 8865 (1987).

[10] M. Ogata and H. Fukuyama, The t-j model for the oxide high-tcsuperconductors, Reports on Progress in Physics **71**, 036501 (2008).

[11] E. Pavarini, *The physics of correlated insulators, metals, and superconductors lecture notes of the Autumn School on Correlated Electrons 2017* (Forschungszentrum Julich GmbH, Julich, 2017).

[12] J. F. Schooley, W. R. Hosler, and M. L. Cohen, Superconductivity in semiconducting srtio$_3$, Phys. Rev. Lett. **12**, 474 (1964).

[13] X. H. Chen, T. Wu, G. Wu, R. H. Liu, H. Chen, and D. F. Fang, Superconductivity at 43 k in SmFeAsO1-xF x, Nature **453**, 761 (2008).

[14] Y. Cao, V. Fatemi, S. Fang, K. Watanabe, T. Taniguchi, E. Kaxiras, and P. Jarillo-Herrero, Unconventional superconductivity in magic-angle graphene superlattices, Nature **556**, 43 (2018).

[15] C. S. Koonce, M. L. Cohen, J. F. Schooley, W. R. Hosler, and E. R. Pfeiffer, Superconducting transition temperatures of semiconducting srtio$_3$, Phys. Rev. **163**, 380 (1967).

[16] X. Lin, Z. Zhu, B. Fauque, and K. Behnia, Fermi surface of the most dilute superconductor, Phys. Rev. X **3**, 021002 (2013).

[17] K. A. Müller and H. Burkard, Srtio$_3$: An intrinsic quantum paraelectric below 4 k, Phys. Rev. B **19**, 3593 (1979).

[18] J. M. Edge, Y. Kedem, U. Aschauer, N. A. Spaldin, and A. V. Balatsky, Quantum critical origin of the superconducting dome in srtio$_3$, Phys. Rev. Lett. **115**, 247002 (2015).

[19] K. Dunnett, A. Narayan, N. A. Spaldin, and A. V. Balatsky, Strain and ferroelectric soft-mode induced superconductivity in strontium titanate, Phys. Rev. B **97**, 144506 (2018).

[20] M. Yi, Y. Zhang, Z.-X. Shen, and D. Lu, Role of the orbital degree of freedom in iron-based superconductors, npj Quantum Materials **2**, 57 (2017).

[21] L. de' Medici and M. Capone, Modeling many-body physics with slave-spin mean-field: Mott and hund's physics in fe-superconductors, Springer Series in Solid-State Sciences , 115–185 (2017).

[22] Y. Wang, C.-J. Kang, H. Miao, and G. Kotliar, Hund's metal physics: From srnio2 to lanio2, Physical Review B **102**, 10.1103/PhysRevB.102.161118 (2020).

[23] Y.-Z. You and A. Vishwanath, Superconductivity from valley fluctuations and approximate SO(4) symmetry in a weak coupling theory of twisted bilayer graphene, npj Quantum Materials **4**, 10.1038/s41535-019-0153-4 (2019).

[24] S. Urazhdin, E. Towsif, and A. Mitrofanov, Orbital entanglement mechanism of superconductivity in strontium titanate (2022), arXiv:2201.04184 [cond-mat.supr-con].

[25] V. Crépel and L. Fu, New mechanism and exact theory of superconductivity from strong repulsive interaction, Science Advances **7**, eabh2233 (2021), https://www.science.org/doi/pdf/10.1126/sciadv.abh2233.

[26] M. Tinkham, *Introduction to superconductivity* (Dover Publications, Mineola, N.Y, 2004).

[27] M. Y. Amusia, K. G. Popov, V. R. Shaginyan, and V. A. Stephanovich, *Theory of Heavy-Fermion Compounds* (Springer International Publishing, 2015).

[28] L. Savary and L. Balents, Quantum spin liquids: a review, Reports on Progress in Physics **80**, 016502 (2016).

[29] J. Bok, *The gap symmetry and fluctuations in high-Tc superconductors* (Kluwer Academic, New York, 2002).

[30] J. E. Hirsch, Spin hall effect, Physical Review Letters **83**, 1834 (1999).

[31] F. D. M. Haldane, Berry curvature on the fermi surface: Anomalous hall effect as a topological fermi-liquid property, Phys. Rev. Lett. **93**, 206602 (2004).

[32] C. E. Matt, D. Sutter, A. M. Cook, Y. Sassa, M. Månsson, O. Tjernberg, L. Das, M. Horio, D. Destraz, C. G. Fatuzzo, K. Hauser, M. Shi, M. Kobayashi, V. N. Strocov, T. Schmitt, P. Dudin, M. Hoesch, S. Pyon, T. Takayama, H. Takagi, O. J. Lipscombe, S. M. Hayden, T. Kurosawa, N. Momono, M. Oda, T. Neupert, and J. Chang, Direct observation of orbital hybridisation in a cuprate superconductor, Nature Communications **9**, 10.1038/s41467-018-03266-0 (2018).

[33] A. M. Oleś, K. Wohlfeld, and G. Khaliullin, Orbital symmetry and orbital excitations in high-tc superconductors, Condensed Matter **4**, 46 (2019).

[34] F. D. M. Haldane, Model for a quantum hall effect without landau levels: Condensed-matter realization of the "parity anomaly", Phys. Rev. Lett. **61**, 2015 (1988).

[35] C. L. Kane and E. J. Mele, Quantum spin hall effect in graphene, Physical Review Letters

95, 10.1103/physrevlett.95.226801 (2005).

[36] L. D. Landau, *Quantum mechanics: non-relativistic theory* (Pergamon Press, Oxford New York, 1977).

[37] D. R. Tilley and J. Tilley, *Superfluidity and Superconductivity* (Routledge, 2019).

[38] D. A. Wollman, D. J. Van Harlingen, J. Giapintzakis, and D. M. Ginsberg, Evidence for $d_{x^2-y^2}$ pairing from the magnetic field modulation of $yba_2cu_3o_7$-pb josephson junctions, Phys. Rev. Lett. **74**, 797 (1995).